Nonlocal Similarity Regularized Sparsity Model for Hyperspectral Target Detection

Zhongwei Huang, Zhenwei Shi, and Shuo Yang

***Abstract*—Sparsity-based approaches have been considered useful for target detection in hyperspectral imagery. Based on the sparse reconstruction theory, the vectors representing the spectral signature of hyperspectral pixels can be a linear combination of linearly dependent training vectors. The training vectors constitute an overcomplete dictionary, which allow for sparse representations for test pixel vectors as only a few of training vectors are used. Such sparsity can be applied in hyperspectral target detection. However, since the sparse decomposition has the potential instability, similar data often have different estimates. In this letter, we propose a nonlocal similarity regularized sparsity model to deal with the problem. Nonlocal similarity enhances classical sparsity model as it preserves the manifold structure of original data and makes more stable estimations for similar data. In addition, the nonlocal sparsity model is effectively solved with a developed greedy algorithm. Experimental results suggest an advantage of the nonlocal sparsity model over conventional sparsity models and a better performance of the proposed algorithm compared with conventional sparsity-based algorithms.**

***Index Terms*—Greedy algorithm, hyperspectral target detection, nonlocal similarity, sparse representation.**

I. Introduction

HYPERSPECTRAL imaging sensors produce a 3-D data structure called data cube with two spatial dimensions and one spectral dimension [10]. The spectrum of each hyperspectral pixel can be viewed as a vector with each entry representing the radiance or reflectance value at each spectral band [9], [10]. In hyperspectral imagery (HSI), different materials normally reflect electromagnetic energy at different and specific wavelength bands. Thus, when detecting a target with a specific material, the target pixels are characterized by unique deterministic spectra [9]. Thus, HSI data are suitable for pixel detection with spectral characteristics [10]. The target detection for HSI is a binary classification problem [5] which aims to label each test pixel as target or background. Several detection algorithms have been developed. Most of them are based on statistics [11]. Among them, adaptive coherence/cosine estimator (ACE) detector, matched filter (MF) [11] detector, and adaptive subspace detector (ASD) [7] are the widely used detectors for hyperspectral target detection.

Recently, sparse signal representation has proven to be a powerful tool in many areas [1], [14]. This success is mainly due to the fact that most natural signals can be sparsely represented by a few coefficients carrying the most important information in a certain dictionary or basis set [14]. The nonzero coefficients are critical since they can determine the category of the signal. To apply the sparsity in HSI target detection directly, a pixelwise sparsity model [5] reconstructs and detects each hyperspectral pixel, respectively. A joint sparsity model [5] is also proposed for HSI target detection, which assumes that the neighboring pixels likely consist of similar materials. Thus, these pixels are sparsely decomposed over a local dictionary simultaneously in joint model. The joint sparsity model suggests a better performance when compared with original pixelwise model.

In contrast to the joint models which consider the similarity of data in local areas, we aim to extend it to a nonlocal fashion. Nonlocal similarity is believed as an important factor in computer vision and image processing [14], defined as repetitive structures and patterns of data in the whole scene of images [2]. This nonlocal similarity is effectively applied in image denoising [2] and image restoration [8]. In HSI processing, target pixels are repetitively and irregularly distributed in the whole image. However, conventional sparsity model fails to preserve such nonlocal similarity [8] which could cause these similar pixels to be decomposed with different sparse coefficients. It will lead to unstable reconstructions and lower detecting performances.

In this letter, we propose a nonlocal similarity regularized sparsity model for target detection in HSI. The model is based on the idea of capturing and preserving the manifold structure of hyperspectral data. We aim to make a more stable and discriminative sparse representation in which similar signals will obtain similar sparse representations. In the proposed model, a constraint is added to preserve the nonlocal similarity of HSI data. A novel greedy algorithm is proposed for solving the model. Most existing algorithms for effective sparse representation are greedy algorithms [1], [12]. In particular, orthogonal matching pursuit (OMP) and simultaneous OMP (SOMP) are used in sparse hyperspectral target detection [5]. We develop the SOMP algorithm in order to effectively solve the proposed model. The proposed algorithm iteratively updates the suboptimal approximation by solving a Lyapunov equation [6]. As the accurate solution to such equation is obtained for each iteration, we find an effective solution to the nonlocal sparsity model.

Manuscript received December 25, 2012; accepted April 30, 2013. Date of publication July 3, 2013; date of current version October 10, 2013. This work was supported in part by the National Natural Science Foundation of China under Grants 61273245 and 91120301, by the 973 Program under Grant 2010CB327904, by the open funding project of the State Key Laboratory of Virtual Reality Technology and Systems, Beihang University, under Grant BUAA-VR-12KF-07, by the Program for New Century Excellent Talents in University of the Ministry of Education of China under Grant NCET-11-0775, and by the Beijing Key Laboratory of Digital Media, Beihang University, Beijing 100191, China.

The authors are with the Image Processing Center, School of Astronautics, Beihang University, Beijing 100191, China (e-mail: zhongweiwong@gmail.com; shizhenwei@buaa.edu.cn; yangshuodf@126.com).

Color versions of one or more of the figures in this paper are available online at http://ieeexplore.ieee.org.

Digital Object Identifier 10.1109/LGRS.2013.2261455

II. Nonlocal-Similarity-Based Sparsity Model for HSI Target Detection

In this section, we first review the existing sparsity models for HSI target detection. Then, we introduce the nonlocal similarity regularized sparsity model which aims to improve the detecting performance by enhancing the stability of sparse representation.

A. Current Sparsity Model for Target Detection

If N pixels form an L-band hyperspectral image $\mathbf{X} = \{\mathbf{x}_i\}_{i=1}^{N} \in \mathbb{R}^{L\times N}$, its each pixel $\mathbf{x}_i, i = 1, \ldots, N$, can be sparsely represented with vectors containing redundant spectral information, which are known as atoms. Each atom is believed as a training sample that belongs to a particular category, i.e., target or nontarget. These atoms constitute an overcomplete spectral dictionary. Denote the spectral dictionary as $\mathbf{D} = [\mathbf{D}_b\ \mathbf{D}_t] \in \mathbb{R}^{L\times M}$, where $\mathbf{D}_b$ and $\mathbf{D}_t$ represent the parts of the dictionary that contain background and target training samples, respectively. Denote $\mathbf{D}_{b_j}, j = 1, \ldots, M_b$, as columns of $\mathbf{D}_b$, and $\mathbf{D}_{t_j}, j = 1, \ldots, M_t$, as columns of $\mathbf{D}_t$, where $M = M_b + M_t$. Then, any given pixel $\mathbf{x}$ can be written as a linear combination of these training samples

$$\mathbf{x} = \sum_{j=1}^{M_b} \mathbf{D}_{b_j} s_{b_j} + \sum_{j=1}^{M_t} \mathbf{D}_{t_j} s_{t_j} = \mathbf{D}_b\mathbf{s}_b + \mathbf{D}_t\mathbf{s}_t = \mathbf{D}\mathbf{s}. \quad (1)$$

The coefficients of reconstruction with background and target training samples, respectively, are denoted with the vector $\mathbf{s} = [\mathbf{s}_b^{\mathrm{T}}\ \mathbf{s}_t^{\mathrm{T}}]^{\mathrm{T}}$.

Supposing that the dictionary of training samples $\mathbf{D}$ is redundant, the coefficient vector $\mathbf{s}$ can be very sparse, containing only a few nonzero entries. Given the test pixel $\mathbf{x}$ and training dictionary $\mathbf{D}$, the classical sparsity model for finding coefficients $\mathbf{s}$ is obtained as [1]

$$(\mathbf{P}_0) : \widehat{\mathbf{s}} = \arg\min \|\mathbf{s}\|_0 \quad \text{subject to } \mathbf{D}\mathbf{s} = \mathbf{x}. \quad (2)$$

However, a tough issue arises as seeking the optimal solution of $(\mathbf{P}_0)$ is nondeterministic polynomial (NP)-hard [1]. Recent methods all give approximate solvers [1]. In particular, greedy pursuit algorithms [1], [12] provide approximate solutions to a relaxed model with fixed sparsity level K_0

$$\widehat{\mathbf{s}} = \arg\min \|\mathbf{D}\mathbf{s} - \mathbf{x}\|_2 \quad \text{subject to } \|\mathbf{s}\|_0 \le K_0. \quad (3)$$

Once the sparse coefficients $\mathbf{s}$ are obtained, we generate a classifier by incorporating a competition between the target subspace and the background subspace. The class of any pixel $\mathbf{x}$ can be determined by

$$\tilde{d}(\mathbf{x}) = \|\mathbf{x} - \mathbf{D}_b\mathbf{s}_b\|_2 - \|\mathbf{x} - \mathbf{D}_t\mathbf{s}_t\|_2 \quad (4)$$

where $\mathbf{s}_b$ and $\mathbf{s}_t$ represent the recovered sparse coefficients corresponding to the background subdictionary $\mathbf{D}_b$ and the target subdictionary $\mathbf{D}_t$, respectively. If $\tilde{d}(\mathbf{x}) > \delta$, where δ is a given threshold, then $\mathbf{x}$ is labeled as a target pixel; otherwise, it is labeled as a background pixel. The nonzero entries of $\mathbf{s}$ are important since they can discriminatively decide whether the test HSI pixel is constructed with background or target training samples.

In addition to pixelwise sparsity model for HSI target detection, a joint sparsity model is proposed [5]. In such model, pixels close to each other in spatial space will be simultaneously reconstructed and detected [5], [13] as pixels in the same neighborhood are believed to consist of similar materials.

B. Nonlocal Similarity Regularized Sparsity Model

In hyperspectral data matrix $\mathbf{X}$, similar spectra representing the same materials are repetitively presented. Recent studies have shown the importance of this nonlocal similarity structure in images [2], [8]. As an unsupervised learning method, sparse decomposition usually fails to maintain the manifold structure of original data [8]. In particular, in dealing with hyperspectral data, spectra belonging to the same class may result in different representing coefficients in the sparse reconstruction process. Such undesired condition can be explained by noise or pixel mixture in hyperspectral scenes. To tackle this problem, we incorporate the assumption that vectors that are similar with each other in the data matrix should have similar sparse representations. In measuring such nonlocal similarity, we use a quadratic constraint with respect to the sparse coefficients

$$\sum_{i=1}^{N} \|\mathbf{s}_i - \sum_j w_{ji}\mathbf{s}_j\|^2 \quad (5)$$

where $\mathbf{s}_i$ represents the sparse coefficients for a data point $\mathbf{x}_i$ and w_{ji} is the weight parameter representing the similarity between $\mathbf{s}_j$ and $\mathbf{s}_i$. For data matrix $\mathbf{X} = [\mathbf{x}_1, \ldots, \mathbf{x}_N]$, the weight matrix $\mathbf{W} = \{w_{ji}\}_{i,j=1}^{N}$ is obtained by

$$w_{ji} = e^{-\frac{\|\mathbf{x}_i - \mathbf{x}_j\|^2}{\sigma}} \quad (6)$$

where σ forces the similarity. When $\mathbf{x}_i$ and $\mathbf{x}_j$ are quite close to each other, w_{ji} will be close to one, and otherwise, we get an output near zero. The constraint in (6) can be transformed by

$$\begin{aligned}\sum_{i=1}^{N} \left\| s_i - \sum_j w_{ji}s_j \right\|^2 &= \|\mathbf{S} - \mathbf{S}\mathbf{W}\|^2 \\ &= \mathrm{Tr}\left(\mathbf{S}(\mathbf{E} - \mathbf{W})(\mathbf{E} - \mathbf{W})^{\mathrm{T}}\mathbf{S}^{\mathrm{T}}\right) \\ &= \mathrm{Tr}(\mathbf{S}\mathbf{M}\mathbf{S}^{\mathrm{T}}) \end{aligned} \quad (7)$$

where $\mathbf{E}$ is the unit matrix and $\mathbf{M} = (\mathbf{E} - \mathbf{W})(\mathbf{E} - \mathbf{W})^{\mathrm{T}}$.

Similar to (3), for a nonlocal sparsity model, we simultaneously deal with all the test pixels in image $\mathbf{X}$, and the sparse constraint is made on the rows of the coefficient matrix $\mathbf{S} = \{\mathbf{s}_i\}_{i=1}^{N} \in \mathbb{R}^{M\times N}$. Then, the problem is defined as

$$\widehat{\mathbf{S}} = \arg\min \|\mathbf{D}\mathbf{S} - \mathbf{X}\|_F \quad \text{subject to } \|\mathbf{S}\|_{\mathrm{row},0} \le K_0 \quad (8)$$

where $\|\cdot\|_F$ denotes the Frobenius norm. In the proposed method, this term is regularized for computational convenience. When adding the constraint in (7) into (8), we obtain the following optimization problem:

$$\begin{aligned}\widehat{\mathbf{S}} = \arg\min &\frac{1}{2}\|\mathbf{D}\mathbf{S} - \mathbf{X}\|_F^2 + \lambda\mathrm{Tr}(\mathbf{S}\mathbf{M}\mathbf{S}^{\mathrm{T}}) \\ &\text{subject to } \|\mathbf{S}\|_{\mathrm{row},0} \le K_0 \end{aligned} \quad (9)$$

where λ is a regularization parameter controlling the level of the nonlocal similarity constraint.

III. Nonlocal-Similarity-Based SOMP

In the proposed method, (9) is solved with a greedy algorithm based on conventional SOMP [4]. As our method incorporates the nonlocal similarity constraint, we denote the proposed algorithm as nonlocal-similarity-based SOMP (NS-SOMP).

The greedy algorithms are believed to be efficient for sparse representation [1], [12]. Generally, greedy algorithms search exhaustively in each iteration to find a suboptimal approximation, by picking the vector that best correlates with the present residual. Recent studies have reported the good performances of greedy algorithms particularly SOMP in dealing with hyperspectral target detection [5]. In each iteration of the SOMP algorithm for solving (3), the index of one atom within $\mathbf{D}$ is picked if it is most close to the current residuals $\mathbf{R}$. Then, the current index set Λ_k is updated by adding this index to it. Then, a suboptimal solution denoted as $\mathbf{P}_k$ is obtained using atoms within the index set which is denoted as $\mathbf{D}_{\Lambda_k}$, and the residuals are updated with the solution. When stopping criterion is met, the sparse representation is obtained using atoms within the final index set Λ approximately by

$$\widehat{\mathbf{S}} = \left(\mathbf{D}_\Lambda^{\mathrm{T}}\mathbf{D}_\Lambda^{\mathrm{T}}\right)^{-1}\mathbf{D}_\Lambda^{\mathrm{T}}\mathbf{X}. \tag{10}$$

To solve the optimization problem in (9) with the greedy algorithm, we first attempt to find an accurate suboptimal solution for each iteration, i.e., we aim to solve the unconstrained problem in kth iteration

$$\widehat{\mathbf{P}}_k = \arg\min \frac{1}{2}\|\mathbf{D}_{\Lambda_k}\mathbf{P}_k - \mathbf{X}\|_F^2 + \lambda \mathrm{Tr}\left(\mathbf{P}_k\mathbf{M}\mathbf{P}_k^{\mathrm{T}}\right). \tag{11}$$

The gradient of $f_{(\mathbf{P}_k)} = (1/2)\|\mathbf{D}_{\Lambda_k}\mathbf{P}_k - \mathbf{X}\|_F^2 + \lambda \mathrm{Tr}(\mathbf{P}_k\mathbf{M}\mathbf{P}_k^{\mathrm{T}})$ can be obtained as

$$\nabla f_{(\mathbf{P}_k)} = \mathbf{D}_{\Lambda_k}^{\mathrm{T}}\mathbf{D}_{\Lambda_k}\mathbf{P}_k - \mathbf{D}_{\Lambda_k}^{\mathrm{T}}\mathbf{X} + \lambda\mathbf{P}_k(\mathbf{M} + \mathbf{M}^{\mathrm{T}}). \tag{12}$$

When forcing the gradient to be zero, we obtain an equation

$$\mathbf{D}_{\Lambda_k}^{\mathrm{T}}\mathbf{D}_{\Lambda_k}\mathbf{P}_k - \mathbf{D}_{\Lambda_k}^{\mathrm{T}}\mathbf{X} + \lambda\mathbf{P}_k(\mathbf{M} + \mathbf{M}^{\mathrm{T}}) = 0 \tag{13}$$

which is actually a Lyapunov equation [6]. Denoting $\mathbf{A} = \mathbf{D}_{\Lambda_k}^{\mathrm{T}}\mathbf{D}_{\Lambda_k}$, $\mathbf{B} = \lambda(\mathbf{M} + \mathbf{M}^{\mathrm{T}})$, and $\mathbf{C} = \mathbf{D}_{\Lambda_k}^{\mathrm{T}}\mathbf{X}$, the Lyapunov equation is obtained as

$$\mathbf{A}\mathbf{P}_k + \mathbf{P}_k\mathbf{B} = \mathbf{C}. \tag{14}$$

Its solution is normally obtained as

$$vec(\mathbf{P}_k) = (\mathbf{E}\otimes\mathbf{A} + \mathbf{B}^T\otimes\mathbf{E})^{-1}vec(\mathbf{C}) \tag{15}$$

where $\mathbf{E}$ still denotes the unit matrix and vec reshapes a matrix columnwise to a vector. The Kronecker product [6] is denoted with $\otimes$. However, the Kronecker product calls heavy consumption for memory, so, in most cases, when matrices $\mathbf{A}$ and $\mathbf{B}$ can be diagonalized, we use the method proposed in [6]. The eigenvalue decompositions of matrices $\mathbf{A}$ and $\mathbf{B}$ are obtained, respectively, as

$$\mathbf{U}^{-1}\mathbf{A}\mathbf{U} = \begin{bmatrix}\alpha_1 & & \\ & \ddots & \\ & & \alpha_M\end{bmatrix} \quad \mathbf{V}^{-1}\mathbf{B}\mathbf{V} = \begin{bmatrix}\beta_1 & & \\ & \ddots & \\ & & \beta_N\end{bmatrix}. \tag{16}$$

Then, the solution $\mathbf{P}_k$ is obtained by

$$\mathbf{P}_k = \mathbf{U}\tilde{\mathbf{P}}_k\mathbf{V}^{-1} \tag{17}$$

where $\tilde{\mathbf{P}}_{k_{ij}} = (\tilde{\mathbf{C}}_{ij}/\alpha_i + \beta_j)$, $i = 1,\ldots,M$, $j = 1,\ldots,N$, and $\tilde{\mathbf{C}} = \mathbf{U}^{-1}\mathbf{C}\mathbf{V}$. Then, we apply the aforementioned method to update the suboptimal solution in each iteration of SOMP. The outline of the proposed algorithm NS-SOMP is given hereinafter:

Algorithm 1 Pseudocode of the NS-SOMP Algorithm.

1: **Input**:
$L \times M$ dictionary $\mathbf{D} = [\mathbf{d}_1 \cdots \mathbf{d}_M]$, $L \times N$ data matrix $\mathbf{X} = [\mathbf{x}_1 \cdots \mathbf{x}_N]$, similarity matrix $\mathbf{M}$, a stopping criterion.
2: Initialization:
iteration: $k = 1$,
initial index set: $\Lambda_0 = \emptyset$,
initial residual: $\mathbf{R}_0 = \mathbf{X}$.
3: Main iteration:
Find the index of atoms that is most close to residuals:
index $\Leftarrow \arg\min_{1\le i\le M}\|\mathbf{d}_i^{\mathrm{T}}\mathbf{R}_{k-1}\|_2$
Update the index set: $\Lambda_k \Leftarrow \Lambda_{k-1}\cup\{index\}$
Compute $\mathbf{P}_k$ with solving the Lyapunov equation:
$\mathbf{P}_k \in \mathbb{R}^{k\times N} \Leftarrow \mathbf{D}_{\Lambda_k}^{\mathrm{T}}\mathbf{D}_{\Lambda_k}\mathbf{P}_k - \mathbf{D}_{\Lambda_k}^{\mathrm{T}}\mathbf{X} + \lambda\mathbf{P}_k(\mathbf{M} + \mathbf{M}^{\mathrm{T}}) = 0$
Update residual: $\mathbf{R}_k \Leftarrow \mathbf{X} - \mathbf{D}_{\Lambda_k}\mathbf{P}_k$
Update iteration: $k \Leftarrow k + 1$
4: Stop if criterion has been met. Otherwise, repeat another iteration.
5: **Output**:
final index set $\Lambda = \Lambda_{k-1}$,
sparse representation $\widehat{\mathbf{S}} = \left(\mathbf{D}_\Lambda^{\mathrm{T}}\mathbf{D}_\Lambda^{\mathrm{T}}\right)^{-1}\mathbf{D}_\Lambda^{\mathrm{T}}\mathbf{X}$.

Once the sparse representation matrix $\widehat{\mathbf{S}}$ is obtained, we could label the pixels in the whole image with the classifier we have introduced in (4).

In order to illustrate the advancement of the proposed model and algorithm on sparse reconstruction, we compare it with conventional pixelwise SOMP on six hyperspectral pixels. The reconstruction results are compared in Fig. 1(a)–(c). The test pixels are randomly extracted from the background pixels in three different positions in the real hyperspectral data displayed in Fig. 2(a). The experiments on the data will be fully explained in Section IV. In order to illustrate the efficiency of the proposed method, we compare the SOMP and NS-SOMP algorithms under the same condition, and it can be seen that the reconstructed data are closer to the original data with the constraint of nonlocal similarity. The relative construction error is also computed as shown in Table I. For a test pixel $\mathbf{x}$, a given spectral dictionary $\mathbf{D}$, and the sparse coefficients $\mathbf{s}$ obtained, we evaluate the construction with a relative error $e(\mathbf{x}) = (\|\mathbf{D}\mathbf{s} - \mathbf{x}\|_2/\|\mathbf{x}\|_2)$. As a better reconstruction will result in a smaller error, the nonlocal similarity constraint enhances the accuracy and stability of the sparse representation in general.

IV. Experimental Results

In this section, we use two real hyperspectral images to demonstrate the efficiency of the nonlocal-similarity-based

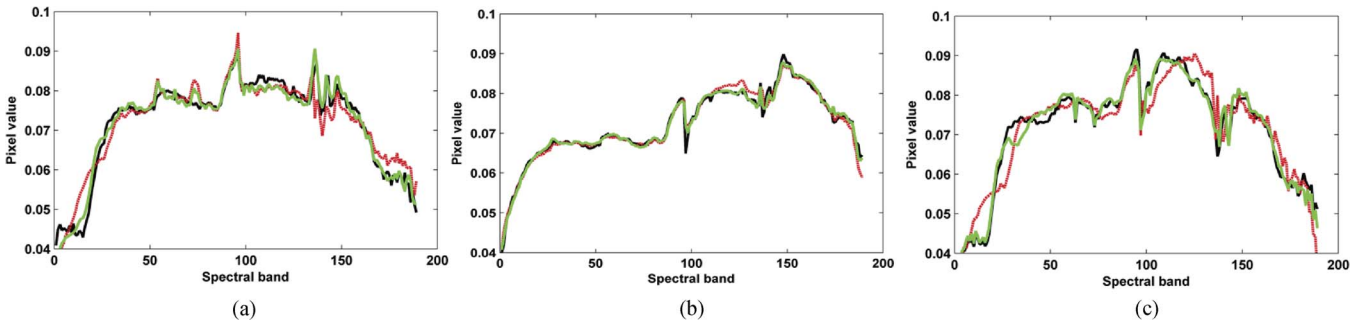

Fig. 1. Sparse reconstruction examples for (black) hyperpspectral data with two algorithms, (red) SOMP and (green) NS-SOMP. For comparison, the reconstructions with the two algorithms are applied with the same sparsity $K_0 = 5$ and based on the same dictionary.

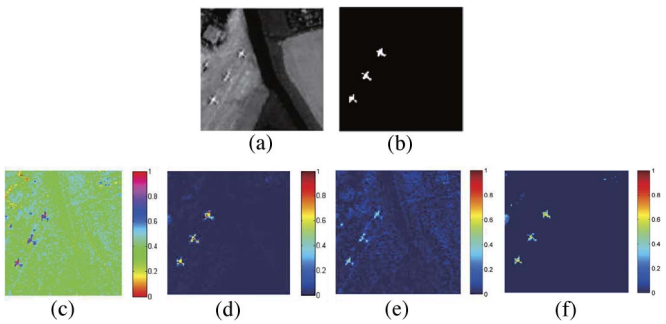

Fig. 2. AVIRIS-I. (a) First band of original hyperspectral data. (b) Ground truth of AVIRIS-I. Detection results for AVIRIS-I with (c) MF, (d) ACE, (e) J-SOMP, and (f) NS-SOMP.

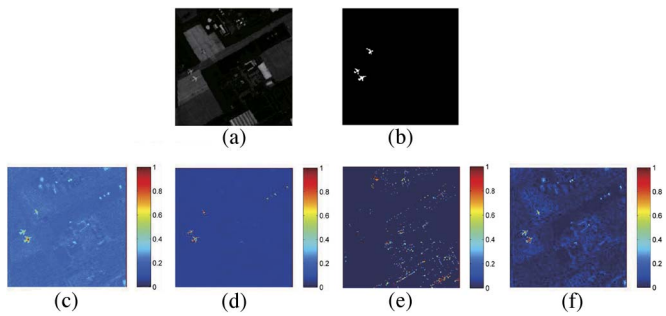

Fig. 3. AVIRIS-II. (a) First band of original hyperspectral data. (b) Ground truth of AVIRIS-II. Detection results for AVIRIS-I with (c) MF, (d) ACE, (e) J-SOMP, and (f) NS-SOMP.

TABLE I
RELATIVE ERRORS OF THE RECONSTRUCTION PROVIDED BY SOMP AND NS-SOMP ARE COMPUTED AND SHOWN IN PERCENTAGES

Error (in percentage)	a	b	c
SOMP	5.29	2.05	6.41
NS-SOMP	2.82	1.34	2.61

sparsity model. In the experiments, the proposed NS-SOMP algorithm is compared with the joint sparsity algorithm [5], pixelwise greedy algorithms SOMP and OMP [13], and three statistics-based algorithms ACE detector, MF detector [11], and ASD [7]. The results of these algorithms are evaluated both visually and quantitatively by the receiver operating characteristic (ROC) curves [3]. The ROC curve is a graphical plot which illustrates the performance of a detector. As the threshold varying in the whole possible region, the ROC curve is generated by plotting the probability of detection (PD) as a function of the probability of false alarms (PFA). PD is calculated by the ratio of the number of target pixels that are labeled as targets and the total number of true target pixels, while PFA is calculated by the ratio of the number of background pixels that are labeled as targets and the total number of pixels. ROC analysis provides tools to compare detectors quantitatively, i.e., the larger the area embraced by the plot, the better the detector performs.

In our experiments, the real hyperspectral images are collected by the Airborne Visible/Infrared Imaging Spectrometer (AVIRIS) sensor. The scenes are two parts of the airport in San Diego, America. The AVIRIS sensor collects the spectral data in 224 bands, and the spectral range is 0.4–2.5 μm. We have removed the water absorption and low signal-to-noise ratio bands, and 189 available bands were left. There are two kinds of airplanes which are detected as targets in two separated images, namely, AVIRIS-I with a size of 100 $\times$ 100 pixels and AVIRIS-II with a size of 200 $\times$ 200 pixels. The first kind of three airplanes is located in the upper left corner of the image, shown in Fig. 2(a). The second kind of three airplanes is located in the lower right corner of the image, shown in Fig. 3(a). For these two images, each pixel on the targets is considered as a target pixel.

For sparsity-based algorithms, the spectral dictionary $\mathbf{D}$ is constructed with two parts: the background subdictionary $\mathbf{D}_b$ and the target subdictionary $\mathbf{D}_t$. For the joint sparsity model used in our experiments, the target subdictionary $\mathbf{D}_t$ is generated by k-means clustering with target pixels, and the number of the cluster centers is set to be ten, as described in [4]. Thus, the target dictionary consists of ten atoms in all. We use the dual-window approach [4] to generate the background subdictionary for the joint sparsity model [5]. The size of the inner windows is set to be 15 $\times$ 15 which is most close to the size of each plane [4], and the size of the outer windows is set to be 25 $\times$ 25; thus, each background dictionary contains 400 atoms in all. The joint sparsity model is solved with SOMP [5] and denoted as J-SOMP in our experiments. For the nonlocal similarity and pixelwise sparsity model-based algorithms, $\mathbf{D}_t$ is the prior knowledge of one spectrum of the targets. Also, a nonlocal background dictionary $\mathbf{D}_b$ is respectively constructed using k-means clustering. The background pixels are clustered into 400 atoms in the background dictionary $\mathbf{D}_b$.

Instead of J-SOMP, all other algorithms in our experiments use the same target of spectrum for detection. Particularly in ASD, it is used to generate the target subspace [7]. The outputs of detectors based on MF, ACE, joint, and nonlocal-similarity-based sparsity model for AVIRIS-I are shown in Fig. 2(c)–(f), respectively, and their outputs for AVIRIS-II

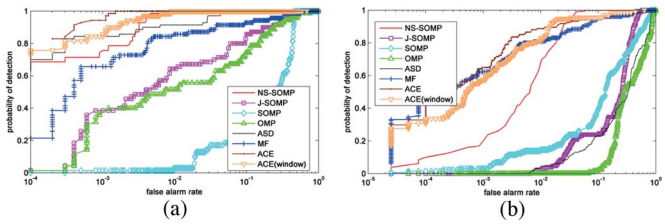

Fig. 4. ROC curves for AVIRIS-I in (a) and for AVIRIS-II in (b) with eight different detection algorithms, respectively: NS-SOMP, J-SOMP, SOMP, OMP, ASD, MF, ACE, and sliding window version of ACE.

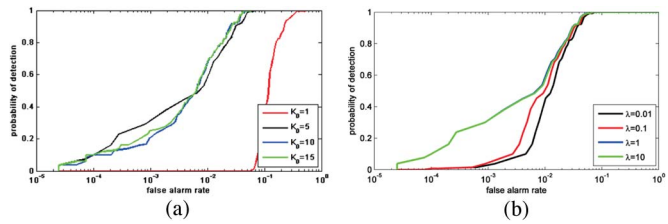

Fig. 5. ROC curves for AVIRIS-II using NS-SOMP with different levels of sparsity K_0 in (a) and different levels of constraint on nonlocal similarity λ in (b).

are shown in Fig. 3(c)–(f), respectively. The outputs are all converted to grayscale images and displayed with false color plots. The color scale bar for each plot is also provided. The ROC curves for AVIRIS-I and AVIRIS-II are displayed in Fig. 4(a) and (b), respectively, with eight different detection algorithms: NS-SOMP, J-SOMP, SOMP, OMP, ASD, MF, ACE, and a sliding window version of ACE. We generate the sliding window version of ACE using the same dual-window approach as J-SOMP does. For AVIRIS-I and AVIRIS-II, we use the same sparsity $K_0 = 10$ for all the sparsity-based algorithms as the stopping criterion. The parameter σ for the similarity constraint in NS-SOMP is set to be one. The performance of most detectors on AVIRIS-I suggests a good performance. Among the sparsity-based algorithms, NS-SOMP performs the best, and J-SOMP also suggests an advantage over pixelwise sparse detectors. Statistics-based algorithms outperform sparsity-based algorithms, and ACE gets the best performance. This is mainly because the scene is relatively small and simple.

In the ROC curves for AVIRIS-II, it can be illustrated that most sparse detectors fail to detect the three planes well. This is because the scene is more complex and could lead to unstable sparse reconstructions. In particular, the joint sparsity model fails to perform well since the dual-window approach may not constitute a qualified background dictionary. In addition, the local similarity can be not effectively applicable under complex conditions. Thus, conventional sparsity model cannot guarantee an accurate representation particularly for the targets. The proposed NS-SOMP detection algorithm is the only sparse method that has good performance for AVIRIS-II, whose ROC curve is higher and more quickly reached to one compared with other sparsity-based algorithms. Compared with ACE and MF, the proposed NS-SOMP falls behind at low false alarm rate but suggests a better performance at high false alarm rate. Such result suggests that, in occasions that we could not afford loss of any targets, the proposed NS-SOMP will become a better alternative to conventional methods.

We also demonstrate the effects of two important factors in NS-SOMP algorithm, i.e., the sparsity K_0 and the similarity constraint parameter λ in (9). We test the performance of the proposed NS-SOMP on AVIRIS-II with different levels of these two parameters and display the ROC curves as shown in Fig. 5(a) and (b). ROC curves in Fig. 5(a) suggest an ascending performance with sparsity K_0 increasing from one to ten, and λ is fixed at one in this experiment. The ROC curves in Fig. 5(b) suggest the importance of incorporating the nonlocal similarity constraint, and K_0 is fixed at ten in this experiment. The performance is also greater with stronger constraint in an appropriate range from $\lambda = 0.01$ to $\lambda = 1$, and the curves representing $\lambda = 1$ and $\lambda = 10$ coincide with each other.

V. Conclusion

In this letter, we have proposed a nonlocal similarity regularized sparsity model for hyperspectral target detection. The model is solved with a novel algorithm called the NS-SOMP. The sparse representation is believed to be unstable in conventional approaches. As nonlocal similarity contains the important manifold structure of the original data, such information is effectively applied in our sparsity model to enhance the stability of sparse representation. Experiments on real hyperspectral data suggest the advancement of the proposed model over existing pixelwise and joint sparsity models. The proposed detection algorithm NS-SOMP also has a better performance than conventional sparse algorithms but is still inferior to ACE, ASD, and even MF in most cases for practical false alarm rates.

References

[1] A. M. Bruckstein, D. L. Donoho, and M. Elad, "From sparse solutions of systems of equations to sparse modeling of signals and images," *Siam Rev.*, vol. 51, no. 1, pp. 34–81, Feb. 2009.

[2] A. Buades, B. Coll, and J. Morel, "A non-local algorithm for image denoising," in *Proc. IEEE Conf. Comput. Vis. Pattern Recognit.*, 2005, vol. 2, pp. 60–65.

[3] C. I. Chang, "Multiparameter receiver operating characteristic analysis for signal detection and classification," *IEEE Sensors J.*, vol. 10, no. 3, pp. 423–442, Mar. 2010.

[4] Y. Chen, N. M. Nasrabadi, and T. D. Tran, "Sparse representation for target detection in hyperspectral imagery," *IEEE J. Sel. Topics Signal Process.*, vol. 5, no. 3, pp. 629–640, Jun. 2011.

[5] Y. Chen, N. M. Nasrabadi, and T. D. Tran, "Simultaneous joint sparsity model for target detection in hyperspectral imagery," *IEEE Geosci. Remote Sens. Lett.*, vol. 8, no. 4, pp. 676–680, Jul. 2011.

[6] A. Jameson, "Solution of the equation AX + XA = C by inversion of an M × M or N × N matrix," *SIAM J. Appl. Math.*, vol. 16, no. 5, pp. 1020–1023, Sep. 1968.

[7] S. Kraut, L. L. Scharf, and L. T. McWhorter, "Adaptive subspace detectors," *IEEE Trans. Signal Process.*, vol. 49, no. 1, pp. 1–16, Jan. 2001.

[8] J. Mairal, F. Bach, J. Ponce, G. Sapiro, and A. zisserman, "Nonlocal sparse models for image restoration," in *Proc. IEEE Int. Conf. Comput. Vis.*, 2009, pp. 2272–2279.

[9] D. Manolakis and G. Shaw, "Detection algorithms for hyperspectral imaging applications," *IEEE Signal Process. Mag.*, vol. 19, no. 1, pp. 29–43, Jan. 2002.

[10] D. Manolakis, D. Marden, and G. A. Shaw, "Hyperspectral image processing for automatic target detection applications," *Lincoln Lab. J.*, vol. 14, no. 1, pp. 79–116, 2003.

[11] D. Manolakis, R. Lockwood, T. Cooley, and J. Jacobson, "Is there a best hyperspectral detection algorithm?" *Algorithms Technol. Multispect., Hyperspect., Ultraspect. Imag. XV*, vol. 7334, no. 1, pp. 733402-1–733402-16, 2009.

[12] J. A. Tropp, "Greed is good: Algorithmic results for sparse approximation," *IEEE Trans. Inf. Theory*, vol. 50, no. 10, pp. 2231–2242, Oct. 2004.

[13] J. A. Tropp, A. C. Gilbert, and M. J. Strauss, "Algorithms for simultaneous sparse approximation. Part I: Greedy pursuit," *Signal Process.—Special Issue Sparse Approximations Signal Image Processing*, vol. 86, no. 3, pp. 572–588, Mar. 2006.

[14] J. Wright, Y. Ma, J. Mairal, G. Sapiro, T. Huang, and S. Yan, "Sparse representation for computer vision and pattern recognition," *Proc. IEEE*, vol. 98, no. 6, pp. 1031–1044, Jun. 2010.